(Received 25 January 2024, Accepted 31 March 2024, Scheduled 13 April 2024)

Application of Improved SROM Based on RBF Neural Network Model in EMC Worst Case Estimation

Bing Hu[2], Yingxin Wang[1,*], Shenghang Huo[2], and Jinjun Bai[2]

[1]*Marine Engineering College, Dalian Maritime University, Dalian 116026, China*
[2]*College of Marine Electrical Engineering, Dalian Maritime University, Dalian 116026, China*

ABSTRACT: The Stochastic Reduced-Order Models (SROMs) are a non-embedded uncertainty analysis method that has the advantages of high computational efficiency, easy implementation, and no dimensional disasters. Recently, it has been widely used in the field of EMC simulation. In the process of optimizing electromagnetic protection design, the worst-case estimation value is an extremely important uncertainty quantification simulation result. However, the SROMs have a large error in providing this result, which limits its application in the field of EMC simulation prediction. An improved SROM based on the Radial Basis Function (RBF) neural network algorithm is proposed in this paper, which improves the fitness function in the genetic algorithm center clustering process and constructs an RBF neural network model to obtain accurate worst-case estimation results. The accuracy improvement effect of the algorithm proposed in this paper in worst-case estimation is quantitatively verified by using a parallel cable crosstalk prediction example from published literature.

1. INTRODUCTION

Uncertainty analysis is a hot research topic in the field of Electromagnetic Compatibility (EMC) in recent years. It treats the input parameters of simulation models as uncertain variables, which can effectively improve the effectiveness of EMC simulation models, explore the probability distribution of the outputs being studied, and confirm the reliability of EMC methods [1].

Uncertainty analysis methods can be divided into two categories based on whether the original solver needs to be modified: embedded and nonembedded. When solving complex EMC problems, it is often necessary to rely on commercial electromagnetic simulation software to simulate the actual electromagnetic environment [2]. However, the vast majority of commercial electromagnetic simulation software companies have not fully opened up the core program of the solver, which leads to embedded uncertainty analysis methods being unable to be used in many cases. The nonembedded uncertainty analysis method does not modify the simulation software solver program, and only a stable deterministic solver is needed to perform normal solving calculations. Compared to the embedded uncertainty analysis method, it is more practical.

Typical nonembedded uncertainty analysis methods include Monte Carlo Method (MCM) [3], Stochastic Collocation Method (SCM) [4], Kriging surrogate model method [5], Stochastic Reduced-Order Models (SROM) [6], etc. MCM is based on the principle of weak law of large numbers and utilizes a large number of discrete sampling points to describe the uncertainty of model parameters. It has unique advantages such as high computational accuracy and easy programming implementation, and is commonly used as a standard result for comparison with other methods [7]. However, the drawback of the MCM is obvious, that is, the principle of weak laws of large numbers determines its extremely slow convergence speed. When the single simulation time is long, the computational resources required by the MCM are almost catastrophic, so the MCM lacks competitiveness in practical engineering applications.

As the generalized polynomial chaos theory gradually improves in the field of computational fluid dynamics, the SCM emerges, which has the dual advantages of high computational accuracy and high computational efficiency. However, as the number of random variables increases, the number of collocation points required by the SCM increases exponentially, and the computational efficiency of the SCM also decreases exponentially, leading to the curse of dimensionality [4, 8].

In order to effectively solve the curse of dimensionality, SROM and Kriging method are widely applied in EMC simulation uncertainty analysis in recent years. SROM is able to produce accurate output statistics by only using a small fraction of the MC computational cost. The idea of the SROM method is essentially different from other methods, but to approximate the statistics of random input variables by using a very small number of selected samples assigned with probabilities. Therefore, unlike MCM looking blindly and exhaustively at all the possible cases, SROM method only needs to examine these selected samples without sacrificing accuracy [9]. SROM has the best applicability and high computational efficiency for stochastic input mathematical models, but it can only provide mean and variance predictions in uncertainty analysis results [6]. The Kriging method uses a small amount of deterministic simulation results as the training set to train the surrogate model, and finally performs a large number of samplings on the input randomness of the model to obtain uncertainty anal-

* Corresponding author: Yingxin Wang (wyxzxmwyx@dlmu.edu.cn).

ysis results. However, its disadvantage is that the accuracy is poor when EMC simulation has large nonlinearity [5].

In the theoretical research of nonembedded uncertainty analysis methods mentioned above, the results are often presented in the form of probability density curves, which focus on the overall accuracy of the proposed or improved algorithms. However, in practical engineering applications, the uncertainty analysis results under the worst-case estimation form have greater significance, that is, the worst protected situation. SROM cannot directly obtain accurate worst-case estimates during uncertainty analysis, which greatly reduces its practicality. In response to this problem, this paper utilizes the RBF neural network model in the field of machine learning to improve the traditional SROM, enabling it to obtain accurate EMC worst-case estimation results and enhancing the competitiveness of the SROM in practical applications. The determination of extreme values is sometimes performed with stratification method, and the controlled stratification method aims at reducing the variance of estimation of extreme quantile, based on a correlated simple model [10, 11], the algorithm proposed in this paper can also provide this simple model for it.

The structure of this paper is as follows. Section 2 introduces the basic principles of the traditional SROM. Section 3 provides a detailed introduction to the implementation process of the improved SROM based on RBF neural network. Section 4 compares the worst-case estimation performance using parallel cable crosstalk examples. Section 5 provides prospects for future research work. Section 6 summarizes the entire text.

2. BASIC PRINCIPLES OF THE TRADITIONAL SROM

When dealing with uncertainty analysis problems, random variables are usually used to model random events, assuming that N random variables $\xi = \{\xi_1, \xi_2, \ldots, \xi_N\}$ are input during EMC simulation. Assuming that H_ξ large number of discrete sampling points need to be utilized by the MCM to describe the uncertainty of model parameters, deterministic EMC simulation is performed on each sampling point $W_i = \{W_{\xi_1}^i, W_{\xi_2}^i, \ldots, W_{\xi N}^i\}$ after sampling to obtain $Y_i = y_{EM}(W_i)$. Finally, after conducting mathematical statistical calculations on Y_i, the EMC uncertainty analysis results and EMC worst-case estimation results can be obtained. When a single EMC simulation takes a long time, the high number of simulations required by this method can lead to low computational efficiency.

When dealing with uncertainty analysis problems, SROM is similar to MCM in that it first uses a large number of discrete sampling points to describe the uncertainty of the model, and the difference is that this method applies genetic algorithm to cluster these discrete sampling points, selects the most representative point as the representative sampling point, and calculates its weight. After deterministic EMC simulation at the representative sampling points is conducted, the mean and variance results can be calculated according to formulas (1) and (2), which are used as the results of EMC uncertainty analysis.

$$E(y) = \sum_{i=1}^{t_\xi} \left[y_{EM}(P_i^{Rep}) \times \omega_i^{Rep} \right] \tag{1}$$

$$\sigma(y) = \sum_{i=1}^{t_\xi} \left\{ \left[y_{EM}(P_i^{Rep}) - E(y) \right]^2 \times \omega_i^{Rep} \right\} \tag{2}$$

Among them, t_ξ is the number of representative sampling points, P_i^{Rep} the representative sampling points, ω_i^{Rep} the weight of the representative sampling points, and y_{EM} the deterministic EMC simulation result of the sampling points.

SROM has the characteristics of high computational efficiency and easy implementation, but it cannot directly provide worst-case estimation results. Based on the properties of Gaussian distribution, the worst-case estimation can be replaced by the form of "mean ± 3 times standard deviation", which is the 99.73% confidence interval boundary point. However, studies have shown that this form introduces significant errors and has poor accuracy in practical applications [12]. The inability to provide accurate worst-case estimates can seriously affect the applicability of SROM in practical applications.

3. IMPROVED SROM BASED ON RBF NEURAL NETWORK MODEL

RBF (Radial Basis Function) neural network is a high-performance three-layer feedforward neural network with good global approximation ability, compact topology, and fast convergence speed [13–15]. RBF neural network model can approximate nonlinear functions arbitrarily and has good generalization ability under the condition of simple network structure. Recently, it is applied in many fields. Its basic idea is to use RBF as the "base" of the hidden unit to form the hidden layer space, and the low-dimensional input vector is transformed into a high-dimensional space through projection, making the originally linearly inseparable problem linearly separable [14]. Figure 1 is a schematic diagram of the basic structure of the RBF neural network.

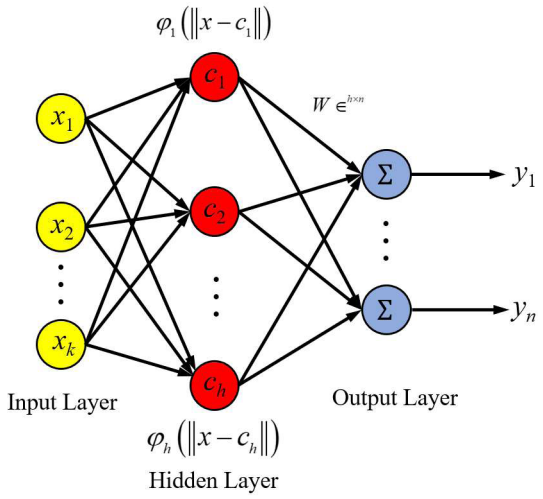

FIGURE 1. Basic structure of RBF neural networks.

An RBF neural network consists of three layers. The first layer is the input layer, which is composed of signal source nodes and only plays a role in transmitting data information without any transformation of input information. The second

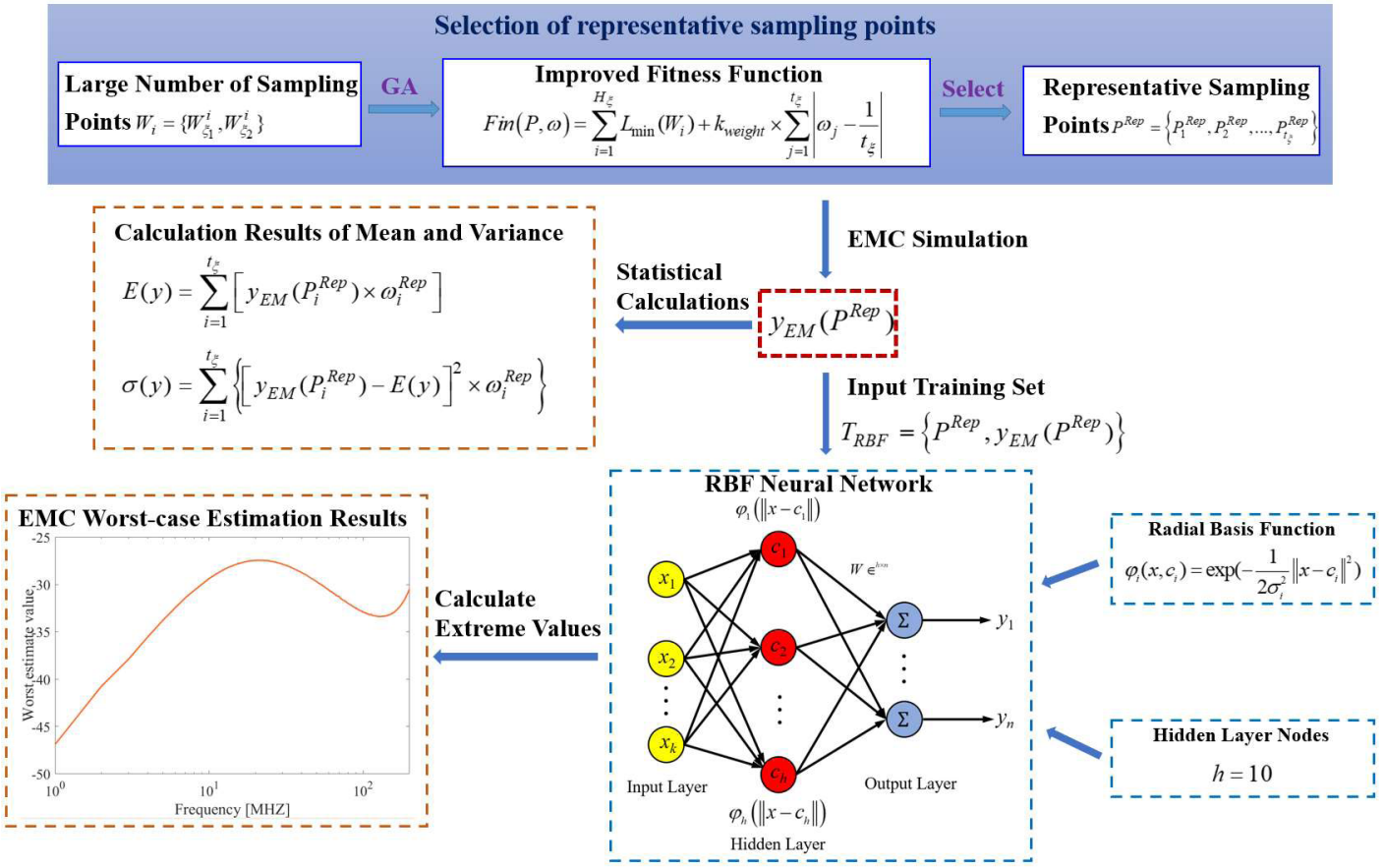

FIGURE 2. The framework of improved SROM based on RBF neural network model.

layer is the hidden layer, which can directly map the input vector to the hidden space without the need for weight connections. Therefore, the connection weight between the input layer and hidden layer is 1, and the number of hidden layer nodes can be determined as needed. The third layer is the output layer, which responds to the input mode. The activation function of the output layer neurons is a linear function. The information output by the hidden layer neurons is linearly weighted and output as the final output result of the entire neural network.

RBF is a real valued function whose value depends only on the distance from the fixed-point c. Any function φ that satisfies the characteristic of $\varphi(x,c) = \varphi(\|x-c\|)$ is a radial basis function, and in simplified cases, it can also be the distance to the origin, which can be expressed as $\varphi(x) = \varphi(\|x\|)$. Usually, Gaussian kernel function is used as the basis function of RBF neural network, and the output of the hidden unit of RBF neural network is:

$$\varphi_i(x,c_i) = G(\|x-c_i\|) = \exp\left(-\frac{1}{2\sigma_i^2}\|x-c_i\|^2\right) \quad (3)$$

Among them, φ is the radial basis function, x the sample, c_i the i-th center point of the kernel function, and σ_i the width of the i-th center point of the function.

The output of RBF neural network is:

$$y_j = \sum_{i=1}^{h} \omega_{ij} \exp\left(-\frac{1}{2\sigma_i^2}\|x_p - c_i\|^2\right), \quad j = 1,2,\cdots,n \quad (4)$$

Among them, y_j represents the output of the RBF neural network, x_p the p-th input sample, c_i the i-th center point, σ_i the width of the i-th center point of the function, ω_{ij} the connection weight coefficient between the hidden layer neuron i and output layer neuron j, h the number of nodes in the hidden layer, and n the number of output samples or classifications.

As introduced in Section 2, the traditional SROM can only obtain mean and variance prediction results when uncertainty analysis is conducted and cannot directly provide accurate worst-case estimation results. Using "mean ± 3 times standard deviation" instead of worst-case estimation results will introduce significant errors. RBF neural network model can approximate nonlinear functions arbitrarily, and the introduction of the hidden layer kernel function concept greatly accelerates its convergence speed and avoids the problem of local extremum [16]. Therefore, using RBF neural networks to improve traditional SROM can solve the problem of its inability to directly provide EMC worst-case estimation results, and the accuracy is guaranteed.

The framework of improved SROM based on RBF neural network model is shown in Figure 2. In order to clearly

illustrate the process and details of the algorithm, the two-dimensional random variable input is used in all the examples in this paper, assuming that it is $\xi = \{\xi_1, \xi_2\}$. The specific steps are as follows:

3.1. Selection of Representative Sampling Points

This paper improves the fitness function when using genetic algorithm for clustering in SROM, so that the weight ω_i^{Rep} of representative sampling points is close to $\frac{1}{t_\xi}$, and the small number of representative sampling points P_i^{Rep} selected through clustering can represent a large number of samples $W_i = \{W_{\xi_1}^i, W_{\xi_2}^i\}$ in the MCM sampling space. The specific steps for selecting representative sampling points are as follows:

Firstly, a large number of samples are taken from the two-dimensional random variable $\xi = \{\xi_1, \xi_2\}$, with a single sampling point in the form of $W_i = \{W_{\xi_1}^i, W_{\xi_2}^i\}$. Among the H_ξ sampling points, t_ξ representative sampling points are randomly selected, and their numbers $\{P_1, P_2, \ldots, P_{t_\xi}\}$ are chromosomes in the genetic algorithm. The Euclidean distance $L(W_i, W_j)$ between two chromosomes is shown in formula (5), and $L(W_i, W_j)$ is used to describe the similarity;

$$L(W_i, W_j) = \sqrt{(W_{\xi_1}^i - W_{\xi_1}^j)^2 + (W_{\xi_2}^i - W_{\xi_2}^j)^2} \quad (5)$$

Secondly, the Euclidean distances between each remaining point in the sampling space and these t_ξ representative sampling points are calculated, and their minimum value is defined as $L_{\min}(W_i)$. The calculation formula is shown in formula (6):

$$L_{\min}(W_i) = \min\{L(W_i, W_{P_1}), L(W_i, W_{P_2}), \ldots, L(W_i, W_{P_{t_\xi}})\} \quad (6)$$

The minimum Euclidean distance is used as the standard to calculate the weight $\{\omega_1, \omega_2, \ldots, \omega_{t_\xi}\}$ of t_ξ representative sampling points in the sampling space. The fitness function of chromosome $\{P_1, P_2, \ldots, P_{t_\xi}\}$ is:

$$Fin\,(P, \omega) = \sum_{i=1}^{H_\xi} L_{\min}(W_i) + k_{weight} \times \sum_{j=1}^{t_\xi} \left| \omega_j - \frac{1}{t_\xi} \right| \quad (7)$$

Among them, $\sum_{i=1}^{H_\xi} L_{\min}(W_i)$ represents the minimum Euclidean distance of all points, and the smaller the value of $\sum_{j=1}^{t_\xi} \left| \omega_j - \frac{1}{t_\xi} \right|$ is, the more average the weights of the selected representative sampling points are. k_{weight} is the proportional coefficient, and the steps to determine k_{weight} are as follows:

1. Let $k_{weight} = 0$ and run the genetic algorithm. At this point, $Fin' = \sum_{i=1}^{H_\xi} L_{\min}(W_i)$ and the value of fitness function Fin' is calculated.
2. The value of parameter Q can be determined by the number of representative sampling points. The range of Q is $0.02 \sim 0.1$. When there are more representative sampling points (more than 100), Q is taken as 0.1. When there are fewer sampling points (less than 10), Q is taken as 0.02. The value of Q is taken proportionally.
3. After obtaining the values of Fin' and Q, the amplitude of k_{weight} can be calculated using $k_{weight} = \frac{Fin'}{Q}$.
4. After the value of k_{weight} is determined, it is substituted into formula (7) to calculate the final fitness function Fin.

Thirdly, through the conventional selection, crossover, and mutation operations of genetic algorithms, the optimal solution $\left\{P_1^{Rep}, P_2^{Rep}, \ldots, P_{t_\xi}^{Rep}\right\}$ for representative sampling points number $\{P_1, P_2, \ldots, P_{t_\xi}\}$ can be obtained, then the final representative sampling point $P^{Rep} = \left\{P_1^{Rep}, P_2^{Rep}, \ldots, P_{t_\xi}^{Rep}\right\}$ and its weight $\omega^{Rep} = \left\{\omega_1^{Rep}, \omega_2^{Rep}, \ldots, \omega_{t_\xi}^{Rep}\right\}$ is obtained.

3.2. Acquisition of EMC Uncertainty Analysis Results

This part is the same as the traditional SROM processing method. After selecting the representative sampling points $P^{Rep} = \left\{P_1^{Rep}, P_2^{Rep}, \ldots, P_{t_\xi}^{Rep}\right\}$ and its weight $\omega^{Rep} = \left\{\omega_1^{Rep}, \omega_2^{Rep}, \ldots, \omega_{t_\xi}^{Rep}\right\}$ using genetic algorithm, deterministic EMC simulation is performed at the representative sampling point to obtain $y_{EM}(P^{Rep})$. Then, the mean and variance results can be calculated using formulas (1) and (2) proposed in Section 2, which are used as the results of EMC uncertainty analysis.

3.3. Acquisition of EMC Worst-Case Estimation Results

In this part, the model parameters of the RBF neural network need to be set first. In this paper, Gaussian kernel function is used as the basis function of the RBF neural network, with the number of hidden layer nodes $h = 10$. The parameters to be learned and optimized in RBF neural networks include the center c_i of the radial basis function, width σ_i, and the connection weight ω_{ij} from the hidden layer to the output layer. The output layer is responsible for optimizing ω_{ij} through a linear optimization strategy, and usually its learning speed is very fast, while the hidden layer needs to use nonlinear optimization methods to adjust the parameters of the activation function. The parameter learning methods of RBF neural networks have different types according to the selection of RBF centers, mainly including self-organizing selection method, random center method, supervised center method, and orthogonal least squares method [16–18].

Because the representative sampling points $P^{Rep} = \left\{P_1^{Rep}, P_2^{Rep}, \ldots, P_{t_\xi}^{Rep}\right\}$ selected by the genetic algorithm

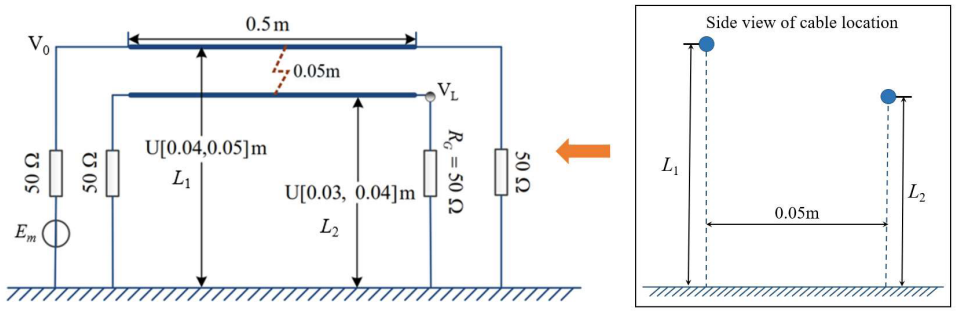

FIGURE 3. Parallel cable crosstalk prediction example considering geometric randomness.

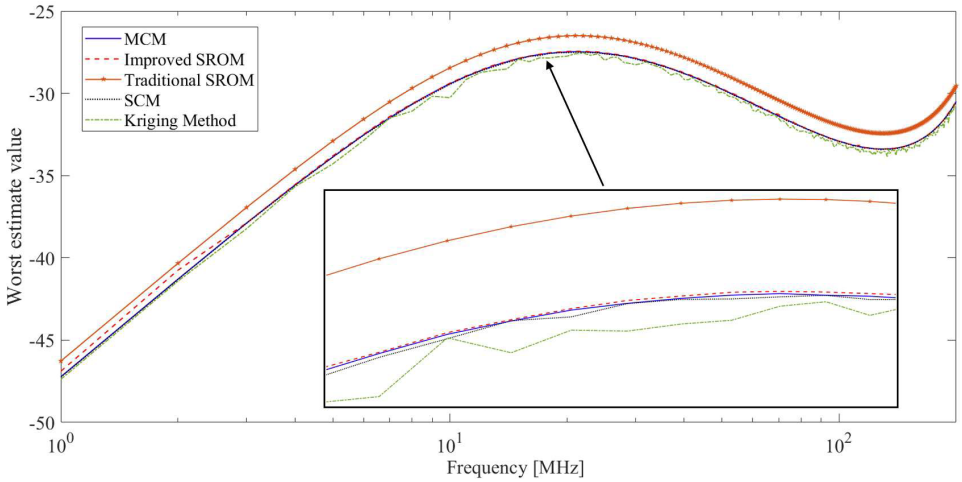

FIGURE 4. Worstcase estimation results for V_{dB}.

can represent a large number of samples $W_i = \{W_{\xi_1}^i, W_{\xi_2}^i\}$

in MCM, t_ξ deterministic EMC simulations $y_{EM}(P^{Rep})$ are performed at the representative sampling points to obtain t_ξ training sets consisting of input-output data pairs $T_{RBF} = \{P^{Rep}, y_{EM}(P^{Rep})\}$, which are used to train the RBF neural network, and the model it constructs is $y_{RBF}(X_i)$. Finally, a large number of samples are taken from the two-dimensional random variable $\xi = \{\xi_1, \xi_2\}$, and the obtained large number of sampling points $K_i = \{K_{\xi_1}^i, K_{\xi_2}^i\}$ are input into $y_{RBF}(X_i)$ to obtain the calculation results $y_{RBF}(K_i)$. The maximum or minimum values that meet the worst-case conditions are selected from $y_{RBF}(K_i)$, which is the accurate EMC worst-case estimation result.

4. PARALLEL CABLE CROSSTALK PREDICTION EXAMPLE CONSIDERING GEOMETRIC RANDOMNESS

The parallel cable crosstalk prediction example considering geometric randomness shown in Figure 3 is used in this section to verify the performance of the improved SROM method based on RBF neural network in EMC worst-case estimation. This example is a standard example from references [19, 20], assuming that the height of parallel cables is an uncertain input parameter, and the example is described by the following random variable model:

$$\begin{cases} L_1(\xi_1) = 0.045 + 0.005 \times \xi_1[\mathrm{m}] \\ L_2(\xi_2) = 0.035 + 0.005 \times \xi_2[\mathrm{m}] \end{cases} \tag{8}$$

Among them, ξ_1 and ξ_2 are uniformly distributed random variables within $[-1, 1]$. The horizontal distance between two cables is 0.05 m. The frequency range calculated in this example is 1 MHz to 200 MHz, and the output result is in decibels of the far end crosstalk voltage V_{dB}. The calculation formula for V_{dB} is as follows.

$$V_{\mathrm{dB}} = 20 \log_{10} \frac{|V_L|}{|V_0|} [\mathrm{dBV}] \tag{9}$$

The deterministic simulation solver for modulus conversion method is implemented in the MATLAB environment in this example, and the parallel cable crosstalk calculation in mature literature is replicated to simulate the capacitance coupling effect and inductance coupling effect between cables, in order to accurately calculate the remote crosstalk voltage. After comparison, the deterministic simulation results are consistent with the results in references [19, 20], ensuring the reliability and representativeness of the results.

Figure 4 shows the worst-case estimation results of V_{dB} for 5 nonembedded uncertainty analysis methods: the improved SROM, MCM, SCM, Kriging method, and traditional SROM.

The MCM conducts 8000 deterministic EMC simulations, and the remaining 4 uncertainty analysis methods all conduct 16 deterministic EMC simulations. The calculation result of the MCM is used as the standard result, and the Feature Selection Verification (FSV) method is used to evaluate the effectiveness of the worst-case estimation results of other uncertainty analysis methods. FSV method is a kind of numerical calculation of the validation rating recommended in IEEE Standard 1597.1, which can give qualitative and quantitative results with regard to the agreement between data sets. It can avoid the subjectivity and non-communicability of human judgment [21, 22]. The evaluation results are shown in Table 1.

TABLE 1. The effectiveness evaluation results provided by FSV method.

Uncertainty analysis method	FSV values
Improved SROM	9.5040×10^{-4}
Traditional SROM	0.0447
SCM	8.6811×10^{-4}
Kriging Method	0.0097

According to the results in Table 1, the traditional SROM has slightly lower accuracy than the other uncertainty analysis methods. Because the traditional SROM cannot directly provide worst-case estimation results, using the "mean ±3 times standard deviation" form results will introduce significant errors, which is not in line with actual engineering situations.

The improved SROM method solves the problem of low computational accuracy in traditional SROM methods, greatly improving its accuracy in EMC worst-case estimation. Meanwhile, as this method does not have the curse of dimensionality, it can still be used normally when the input random variable dimension is high. Compared with SCM, it has stronger applicability and a much faster convergence speed than the MCM and a much higher accuracy in calculating nonlinearity problems than the Kriging method. In summary, the improved SROM method based on RBF neural network model can have 3 advantages: fast calculation speed, high calculation accuracy, and strong applicability.

5. DISCUSSION ON FUTURE RESEARCH WORK

Due to the limitations of the solver, currently only two-dimensional input problems can be solved, so only a simple case can be used to verify the feasibility of the proposed algorithm. When the solver can achieve higher dimensional calculations, complex crosstalk cases that are more realistic will be studied, such as crosstalk calculations in the case of transmission lines being shielded and optical fibers crosstalk. This can expand the applicability of the proposed algorithm, which will become the focus of future work. Because this algorithm is a nonembedded uncertainty analysis method, only a stable solver is needed. Uncertainty analysis can be completed by changing input and output, and it is expected to achieve good results.

6. CONCLUSION

An improved SROM based on RBF neural network model is proposed in this paper to solve the problem of its inability to directly provide accurate worst-case estimation results during uncertainty analysis, thereby improving the applicability of the SROM in practical engineering applications. Firstly, by improving the fitness function of genetic algorithms in traditional SROM for central clustering operations, representative sampling point coordinates with closer weights are selected as much as possible, and they can represent a large number of exhaustive sampling point samples in the MCM sampling space to the greatest extent possible. Secondly, a training set is constructed based on the EMC simulation results at representative sampling points, and an RBF neural network model is trained. Then, exhaustive sampling point samples are input to select the maximum or minimum values that meet the worst-case conditions, as the worst-case estimation result for improved SROM. Finally, in the parallel cable crosstalk prediction example, the worst-case estimation result of MCM is used as standard data, and the effectiveness of the results is quantitatively evaluated using FSV method, verifying that the proposed improvement strategy can achieve EMC worst-case estimation. In summary, compared with other nonembedded uncertainty analysis methods, the improved SROM method based on RBF neural network model has 3 unique advantages: fast calculation speed, high calculation accuracy, and strong applicability. This method is highly competitive in practical engineering applications of electromagnetic protection optimization design.

ACKNOWLEDGEMENT

This work is supported in part by the Youth Science Foundation Project and National Natural Science Foundation of China, under Grant 52301414.

REFERENCES

[1] Manfredi, P., D. V. Ginste, I. S. Stievano, D. D. Zutter, and F. G. Canavero, "Stochastic transmission line analysis via polynomial chaos methods: An overview," *IEEE Electromagnetic Compatibility Magazine*, Vol. 6, No. 3, 77–84, Nov. 2017.

[2] Chen, J., S. Portillo, G. Heileman, G. Hadi, R. Bilalic, M. Martínez-Ramón, S. Hemmady, and E. Schamiloglu, "Time-varying radiation impedance of microcontroller GPIO ports and their dependence on software instructions," *IEEE Transactions on Electromagnetic Compatibility*, Vol. 64, No. 4, 1147–1159, 2022.

[3] Pignari, S. A., G. Spadacini, and F. Grassi, "Modeling field-to-wire coupling in random bundles of wires," *IEEE Electromagnetic Compatibility Magazine*, Vol. 6, No. 3, 85–90, Nov. 2017.

[4] Wang, T., Y. Gao, L. Gao, C.-Y. Liu, J. Wang, and Z. An, "Statistical analysis of crosstalk for automotive wiring harness via polynomial chaos method." *Journal of the Balkan Tribological Association*, Vol. 22, No. 2, 1503–1517, 2016.

[5] Ren, Z., J. Ma, Y. Qi, D. Zhang, and C.-S. Koh, "Managing uncertainties of permanent magnet synchronous machine by adaptive kriging assisted weight index monte carlo simulation method," *IEEE Transactions on Energy Conversion*, Vol. 35, No. 4, 2162–2169, 2020.

[6] Fei, Z., Y. Huang, J. Zhou, and Q. Xu, "Uncertainty quantification of crosstalk using stochastic reduced order models," *IEEE Transactions on Electromagnetic Compatibility*, Vol. 59, No. 1, 228–239, 2016.

[7] Xie, H., J. F. Dawson, J. Yan, A. C. Marvin, and M. P. Robinson, "Numerical and analytical analysis of stochastic electromagnetic fields coupling to a printed circuit board trace," *IEEE Transactions on Electromagnetic Compatibility*, Vol. 62, No. 4, 1128–1135, Aug. 2020.

[8] Cui, C. and Z. Zhang, "High-dimensional uncertainty quantification of electronic and photonic IC with non-Gaussian correlated process variations," *IEEE Transactions on Computer-Aided Design of Integrated Circuits and Systems*, Vol. 39, No. 8, 1649–1661, 2019.

[9] Fei, Z., Y. Huang, J. Zhou, and C. Song, "Numerical analysis of a transmission line illuminated by a random plane-wave field using stochastic reduced order models," *IEEE Access*, Vol. 5, 8741–8751, 2017.

[10] Larbi, M., P. Besnier, and B. Pecqueux, "The adaptive controlled stratification method applied to the determination of extreme interference levels in EMC modeling with uncertain input variables," *IEEE Transactions on Electromagnetic Compatibility*, Vol. 58, No. 2, 543–552, 2016.

[11] Houret, T., P. Besnier, S. Vauchamp, and P. Pouliguen, "Controlled stratification based on kriging surrogate model: An algorithm for determining extreme quantiles in electromagnetic compatibility risk analysis," *IEEE Access*, Vol. 8, 3837–3847, 2019.

[12] Bai, J., X. Geng, and X. Niu, "Application of non-embedded uncertainty analysis methods in worst case estimation of the EMC," *Progress In Electromagnetics Research C*, Vol. 135, 173–180, 2023.

[13] Yu, Z., Z. Qing, and M. Yan, "Application of chaos immune optimization RBF network in dynamic deformation prediction," *Geodesy and Geodynamics*, Vol. 32, No. 5, 53–57, 2012.

[14] Zhang, M.-L. and Z.-H. Zhou, "Adapting RBF neural networks to multi-instance learning," *Neural Processing Letters*, Vol. 23, 1–26, 2006.

[15] Xia, L., P. Hu, K. Ma, and L. Yang, "Research on measurement modeling of spherical joint rotation angle based on RBF–ELM network," *IEEE Sensors Journal*, Vol. 21, No. 20, 23 118–23 124, Oct. 2021.

[16] Yang, Y., S. S. Gao, and G. G. Hu, "Optimal algorithm for RBF neural network structure based on variance significance in output sensitivity," *Control and Decision*, Vol. 30, No. 8, 1393–1398, 2015.

[17] Ye, G., W. Li, and H. Wan, "Study of RBF neural network based on PSO algorithm in nonlinear system identification," in *2015 8th International Conference on Intelligent Computation Technology and Automation (ICICTA)*, 852–855, 2015.

[18] Zhu, G. and X. Wang, "Study on route travel time prediction based on RBF neural network," in *2009 First International Workshop on Education Technology and Computer Science*, Vol. 2, 1118–1122, 2009.

[19] Bai, J., J. Sun, and N. Wang, "Convergence determination of EMC uncertainty simulation based on the improved mean equivalent area method," *Applied Computational Electromagnetics Society Journal*, Vol. 36, No. 11, 1446–1452, Nov. 2021.

[20] Bai, J., G. Zhang, D. Wang, A. P. Duffy, and L. Wang, "Performance comparison of the SGM and the SCM in EMC simulation," *IEEE Transactions on Electromagnetic Compatibility*, Vol. 58, No. 6, 1739–1746, Dec. 2016.

[21] "IEEE Standard for Validation of Computational Electromagnetics Computer Modeling and Simulations," IEEE STD 1597.1-2008, 1–41, 2008.

[22] "IEEE Recommended Practice for Validation of Computational Electromagnetics Computer Modeling and Simulations," IEEE STD 1597.2-2010, 1–124, 2010.